RSC Sustainability

ROYAL SOCIETY OF CHEMISTRY

PAPER

View Article Online
View Journal | View Issue

Cite this: *RSC Sustainability*, 2024, **2**, 1828

Macroalgae-based biochar: preparation and characterization of physicochemical properties for potential applications†

Anjon Kumar Mondal, Cora Hinkley, Lakshmi Krishnan, Nandhini Ravi, Farjana Akter, Peter Ralph and Unnikrishnan Kuzhiumparambil *

Received 10th January 2024
Accepted 12th April 2024

DOI: 10.1039/d4su00008k

rsc.li/rscsus

In this study, we selected five macroalgae species and employed a pyrolysis technique to convert biomass into biochar. Each of the biochar samples was characterized by Scanning Electron Microscopy (SEM), X-ray diffraction (XRD), Fourier transform infrared spectroscopy (FT-IR), thermogravimetric analysis (TGA), Raman spectroscopy, inductively coupled plasma mass spectrometry (ICP-MS) and microwave plasma atomic emission spectroscopy (MP-AES). The physicochemical properties show that the biochar samples from macroalgae are disordered and porous, relatively high in yield, carbon and nitrogen content, ash and pH, and have elevated oxygen-containing functional groups and inorganic minerals (Ca, Na, Mg, K and P). Because of their porous and disordered structures and abundant functional groups, the biochar samples showed an excellent adsorption efficiency of 100, 98.10, 96.78, 98.09 and 95.47% for *Ulva* sp., *Oedogonium* sp., *Asparagopsis*, *Kappaphycus alvarezii* and *Eucheuma denticulatum*, respectively. All biochar samples exhibited negligible amounts of heavy metals (Cd, Cu, Cr, Ni, Pb, As, Zn and Hg), which indicated that biochar is not harmful for plants and crops. The higher ash content in all biochar samples could be advantageous to improve soil quality. Due to the alkaline nature and presence of inorganic minerals, macroalgal biochar could be useful with acidic soil and provide nutritional benefits for crop growth.

Sustainability statement

Biochar, a carbon-rich solid material produced from the pyrolysis of algal biomass has gained substantial attention as a potential solution for sustainable green remediation practices. In the current investigation, all five macroalgae-based biochar samples contain abundant functional groups, higher content of inorganic nutrients (Ca, Na, P, Mg and K), and porous structures. The results achieved from this study indicated that the biochar samples derived from five macroalgae biomass samples have distinguished properties for potential sustainable green applications in many areas, including adsorption, soil fertility for crop growth, catalyst, soil amendment, filler for biocomposites and construction materials and energy storage.

1. Introduction

Biochar is a highly stable carbon-rich porous solid material, one of the critical bioproducts obtained from the thermochemical conversion of biomass in an inert gaseous environment.[1,2] Biochar has attracted significant scientific attention because of its novel properties, such as thermal and mechanical stability, low production cost, uncomplicated manufacturing process, high sustainability, and the widespread availability of feedstock.[3] For this reason, biochar has been identified as a functional material for many applications, such as wastewater treatment, catalyst or catalyst support, soil remediation, incorporation into construction materials as a filler, energy storage (*e.g.*, supercapacitors and batteries) and carbon geosequestration.[4–6] Until now, various types of terrestrial biomass, such as organic wastes, dairy manure, forest and agricultural residuals, have been used to produce biochar.[7] Life cycle analysis (LCA) suggests that biochar has environmental and economic benefits when the residual biomass is converted to biochar.[8] Residual or waste biomass conversion into biochar is a crucial part of the circular bioeconomy, where waste is valorized. Furthermore, transforming organic residuals into biochar prevents GHG emissions released during the organic breakdown of residual biomass and contributes to long-term carbon storage.

It has been recognised that macroalgae are economically and ecologically important, providing indispensable ecosystem services and biomass for nutraceuticals, foods, soil additives and animal feeds.[9] Once the high-value product has been

Climate Change Cluster, University of Technology Sydney, Ultimo, NSW 2007, Australia. E-mail: unnikrishnan.kuzhiumparambil@uts.edu.au

† Electronic supplementary information (ESI) available. See DOI: https://doi.org/10.1039/d4su00008k

removed, the residual biomass can be valorized into biochar. Recently, macroalgae-based biochar production has received increasing attention because of its numerous surface functional groups, high porosity, low production cost, excellent ion exchange capacity, and good aromaticity.[10] These superior properties of macroalgal biochar support its specific utilization, including soil remediation, wastewater treatment, energy storage and as a catalyst.[11,12] Macroalage is used for the bioremediation of wastewater, mainly from aquaculture systems due to their fast growth rates, they can uptake nutrients (N and P) and other elements like heavy metals.[13] Macroalgae is abundant in nature and is commercially cultivated. Biochar production from macroalgal biomass is more sustainable and economical because of its environmentally friendly features and high growth rate than terrestrial biomass. Pyrolysis temperature showed a significant impact on characteristics and phosphate adsorption capability of biochar derived from waste-marine macroalgae (*Undaria pinnatifida* roots).[14,15]

Several techniques, such as pyrolysis, hydrothermal carbonization, gasification, torrefaction and direct combustion, have been used to prepare biochar from macroalgae.[16] Among them, pyrolysis is the most commonly used and feasible technique, which is generally carried out at temperatures between 300 and 1000 °C to convert macroalgal biomass into biochar as a main by-product along with a portion of syngas and bio-oil.[17] The pyrolysis process comprises three major steps: (i) firstly, the loss of moisture content; (ii) the removal of volatile matter and breakdown of organic structures; and (iii) the slow decomposition of residual solids.[18,19] Based on the temperature, heating rate and residence time, it is classified as slow, fast and flash pyrolysis.[20] Slow pyrolysis is much better for producing large quantities of biochar because longer residence time, steady temperature increase and slow degradation of macroalgal biomass resulted in more biochar production than syngas and bio-oil.[21] The porous nature and disordered surfaces of macroalgal biochar improves the availability of nutrients in soil for crops and generates habitats for microorganisms.[22]

The type of feedstock materials and pyrolysis conditions significantly impact the physicochemical properties of macroalgal biochar.[23,24] Shinogi and Kanri (2003) reported significant differences in the yield of biochar prepared through the pyrolysis of different feedstocks.[25] Masek *et al.* (2013) observed that the fixed carbon content increased with the increase of pyrolysis temperature and noted a close relationship between pyrolysis conditions and yield. Fixed carbon content is an indication of resistance of the biochar, which means that the biochar has resistance to either anaerobic or aerobic degradation.[26] Pyrolysis temperature potentially impacts the biochar's abundance of surface functional groups and porous structures.[27] Hossain's group (2011) produced biochar using pyrolysis temperatures between 300 °C and 700 °C.[28] They found that the biochar yield and nitrogenous material decreased with increasing temperature while the mineral content and other trace elements (Mg, Ca, Fe, Cu, Zn and S) increased. The same group also observed alkaline biochar when prepared by high-temperature pyrolysis. On the other hand, low-temperature pyrolysis resulted in acidic biochar.[28] Jung *et al.* pyrolyzed the roots of *Undaria pinnatifida* at the temperature ranging from 200 to 800 °C to evaluate the effect of pyrolysis temperature on biochar properties and phosphate adsorption capacity.[14] It was found that an increase in the pyrolysis temperature led to a decrease of the yield and polarity of biochar and increased the aromaticity. However, ash content almost remained due to carbonization followed by mineralization. The phosphate adsorption capacity was increased, when the pyrolysis temperature was increased to 400 °C. It was also reported that the porosity and surface area increased with the increase of pyrolysis time, however, prolongation of pyrolysis time causes the pores and defects to collapse, which led to the decrease of the surface area of biochar.[29]

Compared to traditional terrestrial biomass-derived biochar, macroalgae-based biochar tends to be relatively low in carbon and have a small surface area; however, it possesses a higher pH value and cation exchange capacity and is often high in phosphorus, nitrogen and inorganic nutrients such as K, Mg, and Ca which could be beneficial to improve chemical properties required for various applications.[30,31] Therefore, preparation techniques and characterizing macroalgae-based biochar's physical and chemical properties is vital in determining their specific applications. In this study, the pyrolysis technique was conducted at 600 °C for 40 min to prepare biochar from five macroalgae species and we systematically investigated their physical, morphological and chemical properties using different analytical methods. To evaluate the potential applications of macroalgae-based biochar, this study presents an overview of the physicochemical properties obtained from five macroalgae species.

2. Materials and methods

2.1. Preparation of biochar from biomass of five macroalgae

Fig. 1 illustrates the preparation process of biochar from five macroalgae species. The five macroalgae species were examined from two taxonomic divisions commonly called greens and reds or Chlorophyta (*Ulva* sp. and *Oedogonium* sp.) and Rhodophyta (*Asparagopsis*, *Kappaphycus alvarezii* and *Eucheuma denticulatum*). Samples were collected from commercial farms in Australia and the Philippines. Samples were washed using deionised water (Milli Q) to remove impurities (*e.g.*, sand, salt *etc.*) and then dried in an oven at 60 °C until constant weight. Subsequently, the dried materials were individually pulverised into a powder using a homemade grinder. A horizontal tube furnace with a quartz tube (Lab Tech, Model STF1200; maximum temperature: 1200 °C) was used for pyrolysis. 40 g of each macroalgae powder was placed in small porcelain boats ($n = 3$) and introduced into the middle of the furnace. Pyrolysis

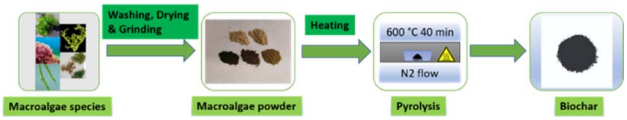

Fig. 1 Schematic diagram of biochar preparation from five macroalgae species.

was carried out at 600 °C for 40 min under a N_2 atmosphere with a temperature ramp rate of 30 °C min^{-1}. N_2 was passed continuously at 4 L min^{-1} for 20 min before heating, during and after the pyrolysis process until the temperature decreased below 100 °C to prevent ignition inside the furnace. The solid mass was then cooled to ambient temperature and collected in plastic jars for further analysis.

2.2. Characterization of biochar samples

A number of experimental analyses were performed to assess the physical and chemical properties of raw macroalgal biomass and the biochar samples. To measure the pH of biochar samples, 1 g of biochar sample was dispersed in 10 mL of MQ water (1W : 10V) and vortexed for 10 min. The percentage biochar yield was determined from the mass of the macroalgal powder and the mass of the biochar after completion of pyrolysis. The ash content was calculated from the mass of each biochar and the mass of the ash at 650 °C for 8 h. Thermogravimetric analysis (TGA) (TA Instrument SDT Q600-1255) was carried out to determine the thermal stability, moisture content and volatile matter of biochar samples. From the TGA curve, the weight loss of biochar samples determined the moisture content after the samples were heated to 110 °C under a N_2 atmosphere. The weight loss determined the volatile matter after the biochar samples were heated to 900 °C. Fixed carbon (FC) was calculated by using the following formula:[32]

$$\text{FC (wt\%)} = 100 - (\text{moisture content wt\%} + \text{volatile matter wt\%} + \text{ash content wt\%})$$

Cellulose, hemicellulose and protein content were determined using the NREL protocol and published reports.[33–35] A CN analyser (LECO 630-300-400) was used to analyze the percentages of C and N and C : N ratio. The elemental composition and heavy metals were analysed using MP-AES (Agilent Technologies 4210 MP-AES) and ICP-MS (Agilent Technologies 7700 ICP-MS), respectively. The surface functional group of biochar samples was determined using a Fourier transform infrared spectrometer in the ATR mode (Nicolet FT-IR 6700). The spectra were recorded from a range of 4000 to 400 cm^{-1} wavelength. The surface morphology of each raw biomass and biochar was observed using scanning electron microscopy (Zeiss EVO LS15) coupled with energy-dispersive X-ray spectroscopy. X-ray diffraction (Bruker D8 DISCOVER) was employed to determine the crystalline structure of biochar samples. The samples were scanned in the range of 2θ from 10 to 80° with a scan speed of 5° min^{-1}. Raman Spectroscopy (ThermoScientific DXR3 SmartRaman) was employed to determine the structural evaluation of biochar samples at an excitation wavelength of 532 nm.

2.3 Adsorption experiments

Batch adsorption experiments were carried out to evaluate the adsorption efficiency and adsorption capacity for five macroalgal biochar samples. For this purpose, a stock solution was prepared by dissolving 1 mg of methylene blue (MB) in 1 Litre MQ water (1 mg L^{-1}). 200 mg of each biochar sample was added to 100 mL stock solution containing five different conical flasks and placed on a reciprocating shaker at 150 rpm for 6 h. After 6 h, all five solutions were filtered by using a 0.20 μm syringe filter. The concentrations of MB solutions were determined using a UV/vis spectrophotometer (Agilent Technologies, Cary 60) at the wavelength of 664 nm. The adsorption efficiency and adsorption capacity can be calculated by using the following equations:[36]

$$\text{Adsorption efficiency (\%)} = (C_0 - C_e)/C_0 \times 100 \quad (1)$$

$$\text{Adsorption capacity } (q_e) = (C_0 - C_e) \times \text{V m}^{-1} \quad (2)$$

3. Results and discussion

The basic information on the physical and chemical properties of all macroalgal biomass samples is presented in Table 1. Most of the macroalgal biomass samples show a relatively low carbon content (21.42–39.20%), high nitrogen content (0.65–6.28%) with the C : N ratio ranging from 6.25% to 39.58%. As shown in Table 1, cellulose, hemicellulose and protein content also varies with macroalgae species. Compared to lignocellulosic biomass such as wood, the low carbon content is typical of many macroalgae-based biomass and is due to the comparatively high ash content.[37,38]

Macroalgal biochar's physical and chemical properties play an important role in evaluating its possible applications. The biochar samples derived from five macroalgal species display a wide range of physical and chemical properties, summarized

Table 1 Physicochemical properties of five macroalgal biomass

Parameters	Units	*Ulva* sp.	*Asparagopsis*	*Oedogonium* sp.	*Kappaphycus alvarezii*	*Eucheuma denticulatum*
Ash	%	9.11	12.87	3.75	17.91	24.34
Moisture content	%	7.43	5.4	7.02	9.04	7.83
Volatile matter	%	65.49	65.09	71.56	61.45	63.87
Carbon (C)	%	31.45	32.02	39.20	25.69	21.42
Nitrogen (N)	%	2.06	3.34	6.28	0.65	0.96
C : N ratio		15.28	9.59	6.25	39.58	22.42
Cellulose	%	1.68	13.98	56.04	22.76	12.16
Hemicellulose	%	2.37	16.62	Not detected	41.34	27.20
Protein	%	12.93	20.97	39.43	4.08	6.02

Table 2 Physicochemical properties of biochar obtained from five macroalgal biomass samples

Parameters	Units	*Ulva* sp.	*Asparagopsis*	*Oedogonium* sp.	*Kappaphycus alvarezii*	*Eucheuma denticulatum*
Yield	%	30.46	40.0	28.2	41.59	46.96
Ash	%	31.1	30.86	12.6	41.73	52.12
pH		10.53	9.74	10.95	10.42	9.86
Moisture content	%	3.62	2.43	3.97	1.99	1.33
Volatile matter	%	22.87	34.21	14.57	31.34	43.92
Fixed carbon (FC)	%	42.41	32.5	68.86	24.94	2.63
Carbon (C)	%	55.77	51.89	70.23	52.23	40.12
Nitrogen (N)	%	3.78	4.97	7.91	0.99	1.50
C : N ratio		14.74	10.44	8.87	52.60	26.79
Oxygen (O)	%	38.53	30.30	22.56	28.71	28.32
Sulfur (S)	%	4.18	12.57	0.09	13.24	15.79
Ca	g kg^{-1}	247.64	210.04	127.94	42.61	22.07
Na	g kg^{-1}	160.00	177.27	48.95	78.52	66.81
K	g kg^{-1}	90.13	113.94	90.78	448.38	326.98
Mg	g kg^{-1}	121.83	9.54	5.57	10.42	31.86
P	g kg^{-1}	49.19	56.40	48.63	52.45	48.42
Fe	g kg^{-1}	1.75	0.74	0.13	1.24	0.74
Si	g kg^{-1}	1.23	1.13	0.14	0.67	0.52

in Table 2. The samples showed significant variations along with some common properties. In general, these properties of biochar depend on the type of macroalgal biomass and pyrolysis conditions. Some previous studies show that the macroalgal biochar quality in terms of yield, pH, structural morphology, ash content, carbon and nitrogen content and inorganic nutrients varies with pyrolysis temperature.[23,39] All biochar samples produced at 600 °C and a residence time of 40 min show moderate yield ranging from 28.2% to 46.96% and high ash content widely ranging from 12.6 to 52.12%, compared to pine wood-derived biochar.[40] The produced bio-oil and gas along with the biochar was obtained through mass balance calculation using eqn (1), (2), S1 and S(4) (ESI).† The percentage of yield for biochar, bio-oil and gas are presented in Table S2 (ESI).† The bio-oil obtained from five macroalgae species ranged between 6.37% and 9.06%, while the gas content ranges from 46.17% to 63.17%. The carbon content of the macroalgae was relatively higher for all biochar samples, between 40.12% and 70.23%, which is higher and comparable with biochar derived from many livestock manure and lignocellulosic biomass.[39] As depicted in Table 2, all biochar samples showed alkaline characteristics. The biochar pH from five macroalgae species ranged from 9.74 to 10.95. The fixed carbon content ranges between 24.94% and 68.86% in all biochars except *Eucheuma denticulatum* (2.63%). A comparison of different parameters for five macroalgae-based biochar samples and biochar obtained from various lignocellulosic biomass and livestock manure is presented in Table S3 (ESI).† It was reported that macroalgal biochar's carbon content and yield are comparatively lower than those of lignocellulosic biochar; however, they are higher in ash content, pH and inorganic nutrients, such as Na, Ca, Mg, K and P.[41,42] It has been shown that the carbon content and yield gradually increase with increasing pyrolysis temperature and residence time while decreasing when the temperature rises from 300 °C to 750 °C and 10 to 60 min[40,43] The inorganic metal ions combine with the hydroxyl and aldehyde groups present in macroalgal biomass samples forming a metal ion–water complex, which act as a catalyst to induce the dehydration reaction during the pyrolysis and changes the elemental composition and other properties in biochar.[44,45]

As presented in Table 2, the biochar samples exhibited high nitrogen content (0.99–7.91%) and inorganic nutrients; in particular, the amount of Na, Ca, Mg, K and P was relatively high (5.57–448.38 g kg^{-1}) in all samples. In contrast, the amount of heavy metals, including Cd, Cu, Cr, Ni, Pb, As, Zn and Hg, was very low as shown in Table 3 compared to lignocellulosic biochar.[46]

Scanning electron microscopy examined the surface morphologies and microstructure of these five macroalgal biomass and biochar samples. The SEM images of the five biomass and biochar samples (pyrolysed at 600 °C) are presented in Fig. 2. Biochar samples showed different physical appearances from their respective biomass samples. Compared to the regular structure of macroalgal biomass, the surface of all biochar samples exhibited rough and porous structures.

These irregular shapes with cavities and porous structures consisting of micro and macro-pores were developed due to the rapid release of volatile organic matter from the biomass during the pyrolysis.[47] Generally, macroalgal biochar exhibits a lower surface area compared to biochar derived from lignocellulosic sources.[48] However, previous studies have indicated that the surface area tends to slightly increase with higher pyrolysis temperatures. The presence of numerous pores and defects on the surface of all macroalgal biochar samples may contribute to a higher effective surface area.[13] These porous and irregular surface features are advantageous for the adsorption of pollutants from wastewater, as highlighted in the literature.[36]

Thermogravimetric analysis was conducted at a heating rate of 10 °C in a nitrogen environment from 25 to 900 °C to study the thermal characteristics of raw macroalgal biomass samples

Table 3 Heavy metal contents in five biochar samples

Heavy metal	Units	*Ulva* sp.	*Asparagopsis*	*Oedogonium* sp.	*Kappaphycus alvarezii*	*Eucheuma denticulatum*
Cd	mg kg^{-1}	0.07	0.07	0.05	0.062	1.23
Cu	mg kg^{-1}	1.03	0.48	0.14	4.10	0.70
Cr	mg kg^{-1}	1.63	2.07	0.35	12.83	11.60
Ni	mg kg^{-1}	1.14	7.15	1.37	9.02	5.22
Pb	mg kg^{-1}	8.14	4.22	4.12	1.76	5.24
As	mg kg^{-1}	0.61	0.45	0.05	0.37	0.99
Zn	mg kg^{-1}	67.86	50.76	44.90	79.86	46.88
Hg	mg kg^{-1}	0.15	0.38	0.26	0.08	0.08

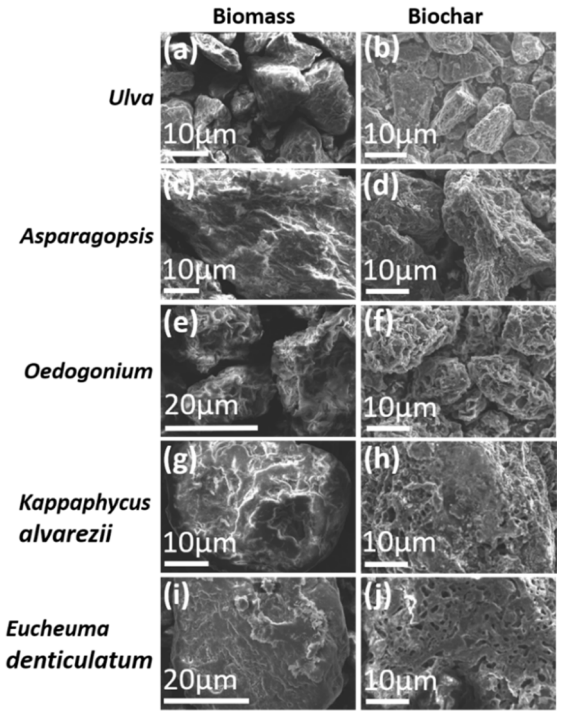

Fig. 2 SEM images of 5 macroalgal biomass and biochar samples: *Ulva* sp. (a) biomass, (b) biochar; *Asparagopsis* (c) biomass (d) biochar; *Oedogonium* sp. (e) biomass, (f) biochar; *Kappaphycus alvarezii* (g) biomass (h) biochar; *Eucheuma denticulatum* (i) biomass (j) biochar.

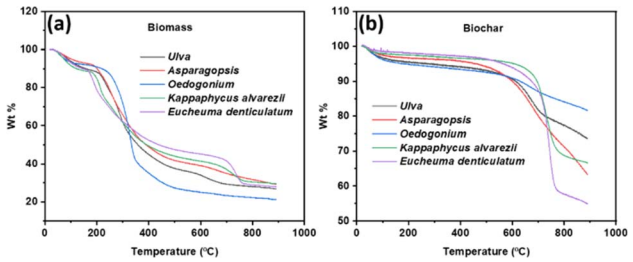

Fig. 3 TGA curves of (a) macroalgal biomass and (b) biochar.

and their derived biochar. Fig. 3 represents the TGA curves of five macroalgal biomass and biochar samples. As shown in Fig. 3(a), all macroalgal biomass samples were less thermally stable than the biochar samples, which is associated with the thermal degradation of organic compounds.[49] The macroalgal biomass was decomposed in three steps. The first step of decomposition and the weight loss from room temperature to 200 °C is related to removing the moisture content and releasing a small amount of volatile matter.[50] The primary weight loss occurred in the second decomposition step from 200 °C to 500 °C, corresponding to the combustion of organic compounds such as proteins, carbohydrates and lipids.[51] In the third step, the weight loss is attributed to the combustion of solid carbonaceous structures.[52]

Fig. 3(b) shows the TGA curves of macroalgal biochar samples, which were quite different from the raw biomass samples and burned in only two steps. The main reason for the differences between TGA curves of biomass and biochar samples is the degradation of protein, carbohydrate, and lipid during the pyrolysis of raw macroalgal biomass. In the first step, a moderate weight loss was observed in all biochar samples until the temperature reached around 600 °C, indicating the removal of moisture adsorbed on the biochar surface. The weight loss between the temperature range of 600 °C and around 780 °C in the second step is due to the further combustion of carbon-rich solids.[53]

The XRD patterns of macroalgal biomass and respective biochar samples are presented in Fig. 4. The XRD patterns of all biomass samples in Fig. 4(a) and (c) show a few broad diffraction peaks with low intensities, indicating the low crystallinity and amorphous nature of carbon.[10] However, the intact structure of raw algal biomass was disintegrated upon pyrolysis at 600 °C and created a number of sharp peaks, indicating the higher crystalline nature of biochar samples shown in Fig. 4(b) and (d). The XRD pattern of macroalgae-derived biochar samples shows numerous peaks of mineral phases. Several sharp peaks appeared in the region at $2\theta = 20$–$30°$ in different biochar samples, ascribed to various inorganic components (CaO, SiO_2 and MgO) and stacked graphitic layer.[54] The diffraction peaks observed at 2θ between 30° and 70° indicate the presence of minerals in $CaCO_3$, $MgCO_3$, $Ca_3(PO_4)_2$, NaCl, KCl, Fe_3O_4 and FeS.[55–57] The peaks located at 26–28° and around 43° in all biochar samples correspond to the (002) crystal plane of crystalline carbon, indicating the existence of graphitic structures.[36]

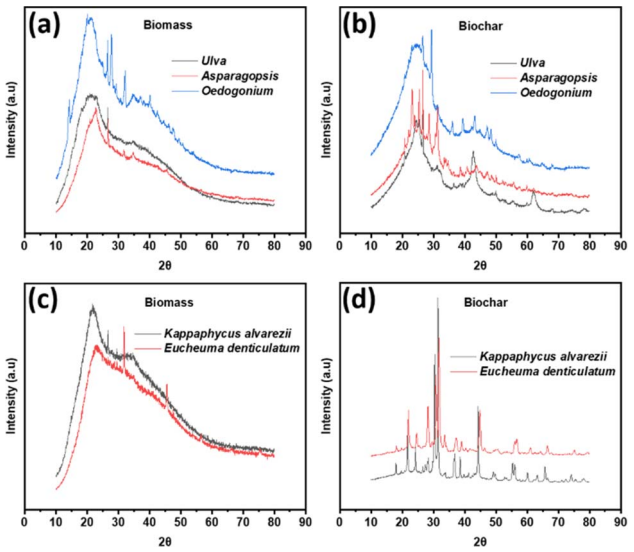

Fig. 4 X-ray diffraction patterns of (a) biomass (*Ulva* sp., *Asparagopsis* and *Oedogonium* sp.), (b) biochar (*Ulva* sp., *Asparagopsis* and *Oedogonium* sp.), (C) biomass (*Kappaphycus alvarezii* and *Eucheuma denticulatum*) and (d) biochar (*Kappaphycus alvarezii* and *Eucheuma denticulatum*).

FTIR was performed to identify functional groups in macroalgal biomass and their derived biochar samples. The spectra of different biomass and biochar samples are shown in Fig. 5. As shown in Fig. 5(a), two broad peaks appeared at around 3340 cm^{-1} and 2927 cm^{-1} in all biomass samples, representing an –OH group (alcoholic and phenolic) and methyl C–H stretching, respectively. These two peaks disappeared from biochar samples (Fig. 5(b)) due to the breakdown of these polymeric structures on pyrolyzing at 600 °C.[56] The carbonyl C=O stretching vibration was observed near 1645 cm^{-1}, 1153 cm^{-1} and 1030 cm^{-1} in biomass samples (Fig. 5(a)). After preparation of biochar, the peak at 1153 cm^{-1} was eliminated from all biochar samples (Fig. 5(b)). A narrow peak of C=O group was found at 1690 cm^{-1} in the spectra of biochar from *Ulva* sp. and *Asparagopsis*, while an intense peak of C=O stretching in the carboxyl group appeared at 1096 cm^{-1} in all five biochar samples (Fig. 5(b)). The presence of the carboxyl group on biochar increases the adsorption capacity of heavy metals.[58]

The loss of specific peaks in biochar samples indicated the loss of functional groups with increased pyrolysis temperature. At high temperatures (600 °C), aliphatic structures are transformed into aromatic structures with more phenolic groups, which results in the disappearance of some bands and the appearance of new bands with less intensity and the formation of graphitic structures in biochar samples.[36,54] The band at 1425 cm^{-1} in Fig. 5(a) was due to the $-CH_3$ and $-CH_2^-$ groups, demonstrating the presence of alkanes and a band located at around 1230 cm^{-1} was ascribed to the C–O–C stretching (phenolic deformation).[59] A band at 1590 cm^{-1} in all biochar spectra in Fig. 5(b) represents aromatic C=C stretching.[36] The peak at 851 cm^{-1} in biomass samples (Fig. 5(a)), around 873 cm^{-1} in the spectra of biochar from *Oedogonium* sp., *Kappaphycus alvarezii* and *Eucheuma denticulatum* (Fig. 5(b)) and at 800 cm^{-1} in biochar samples (Fig. 5(b)) were assigned to the deformation of aromatic C–H bending.[60] The 612 cm^{-1} and 412 cm^{-1} bands in Fig. 5(b) belonged to C–C stretching.[57]

Raman spectroscopy was employed for further assessment of the structure of macroalgal biomass and biochar, which is shown in Fig. 6. Raman spectra of biochar comprise two prominent bands: G band (1560–1610 cm^{-1}) and D band (1320–1380 cm^{-1}). The D band is associated with the distorted amorphous graphitic structure, while the G band can be ascribed to the graphitic crystalline structure.[57] Fig. 6(a) shows no visible D and G bands in all raw biomass samples. However, macroalgal biochar showed obvious D bands between 1361 cm^{-1} and 1375 cm^{-1} and G bands ranging from 1578 cm^{-1} to 1580 cm^{-1} (Fig. 6(b)). The intensity ratio of D and G bands (I_D/I_G) determines the graphitic degree of carbon.[61] The higher I_D/I_G ratio indicates the large amount of defects and disorder.[62] In this study, all biochar samples showed a relatively higher I_D/I_G ratio ranging from 0.91 to 1.11, which might demonstrate a disordered and defective structure of biochar samples. The higher I_D/I_G ratio value at the increased pyrolysis temperature was also reported earlier.[63,64]

A range of elemental analytical techniques were used to analyse biochar samples obtained from five macroalgal biomass samples. Fig. 7 depicts the variation of inorganic nutrients and heavy metals present in biochar samples. As discussed above, all five macroalgae-based biochar samples comprise a higher content of inorganic nutrients (Ca, Na, P, Mg and K), but this varies between species shown in Fig. 7(a). The higher inorganic nutrients and high pH value could provide substantial nutritional benefits to soils and the productivity of crops and are likely to be suitable to apply for acidic soils. The macroalgal

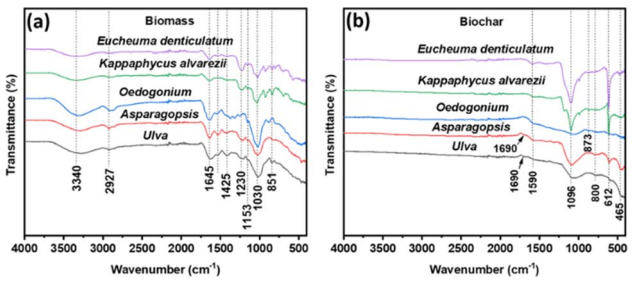

Fig. 5 FTIR spectra of (a) macroalgal biomass and (b) prepared biochar samples at 600 °C.

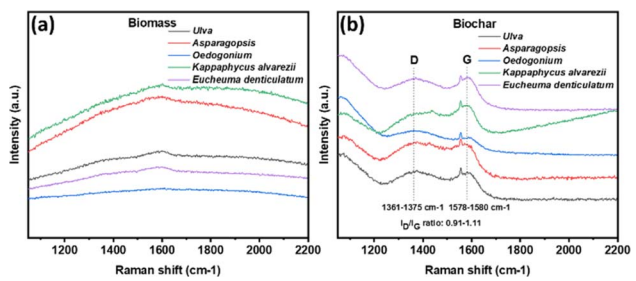

Fig. 6 Raman spectra of (a) macroalgal raw biomass and (b) prepared biochar pyrolysed at 600 °C.

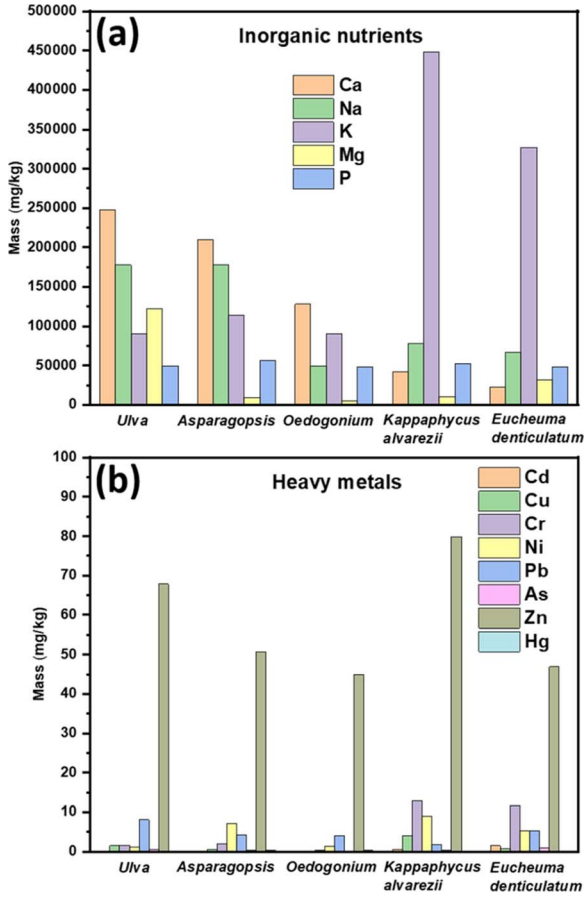

Fig. 7 Variation of (a) inorganic nutrients and (b) heavy metals present in biochar samples.

biochar exhibited high ash content, which is beneficial in soil amendment.[65]

Another advantage of the five biochar samples in this study is the presence of abundant functional groups and porous structures, which could increase the adsorption capacity of heavy metals and other pollutants from wastewater.[66] We have conducted adsorption experiments to observe the adsorption behaviour of five macroalgae-based biochar samples and the adsorption efficiency and adsorption capacity are presented in Table S4 (ESI).†

Because of their porous and irregular structures and abundant functional groups, biochar samples obtained from *Ulva* sp., *Oedogonium* sp., *Asparagopsis*, *Kappaphycus alvarezii* and *Eucheuma denticulatum* showed an excellent adsorption efficiency of 100%, 98.10%, 96.78%, 98.09% and 95.47%, respectively. Due to the high adsorption efficiency and reusability of macroalgae based biochar also reported earlier, all macroalgae derived biochar in this study can be considered as a low cost promising alternative adsorbent to expensive activated carbon for waste water treatment in the textile industry.[36]

As mentioned in the description of FTIR spectra (Fig. 5), aliphatic structures are transformed into aromatic structures at increased temperature. Aromatic functional groups provide more heterogeneous adsorption sites and play an important role in the adsorption of organic contaminants and a positive relationship between aromaticity and adsorption affinity has been reported.[67] The presence of various aromatic functional groups in all biochar samples in this work may be advantageous in removing organic contaminants from the waste water.[68]

Because of their hierarchical structure, eco-friendly nature, chemical inertness and good thermal and mechanical stability, macroalgae-based biochar is being considered as an excellent catalyst for biodiesel production *via* the transesterification process.[69] The inorganic minerals (Ca, Mg, Fe, K *etc.*) present in the biochar enhance the catalytic activity of biochar catalysts. The functional groups on the surface of biochar also act as catalysts during pyrolysis.[56] In the current study, all macroalgae derived biochar samples contain available inorganic minerals and various functional groups. Those properties could make biochar a sustainable catalyst for biodiesel production.[69]

Currently, biochar is considered as a bio-based filler instead of existing synthetic materials in composite manufacturing and construction materials due to its renewable nature, excellent thermal stability, low production cost and insignificant adverse impact on the environment.[70] The surface functional groups present in the biochar play a vital role in the interlocking of the composite and construction materials and the biochar enhances the thermal stability and mechanical strength of composites.[71] The presence of available functional groups in five macroalgal biochar samples could make them suitable fillers for bio-composites and construction materials.[72]

Moreover, the porous and disordered structure of the prepared biochar can increase soil water retention, improving the effectiveness of water use on crops and plants .[73] These structural characteristics of macroalgae biochar also make them favourable as electrode materials for energy storage devices, particularly for supercapacitors.[74] All biochar samples in this investigation present a relatively higher carbon (40.12–70.23%) and nitrogen (0.99–7.91%) content, which is higher than that of biochar obtained from poultry litter and dairy manure[75,76] and comparable with some of the lignocellulosic biochar.[39] The excessive amount of heavy metals (Cd, Cu, Cr, Ni, Pb, As, Zn and Hg) in various biochar harms crops and plant growth.[30] Remarkably, all biochar samples obtained from the five macroalgae biomass samples in this study showed negligible heavy metals (Fig. 7(b)), which contentedly meet the specification set by International Biochar Initiative (IBI) Biochar Standards and European Biochar Certificate-Guidelines for a Sustainable Production of Biochar.[77,78]

4. Conclusions

We successfully prepared a series of macroalgae-based biochar samples and a comprehensive investigation was carried out using various experimental techniques. The results achieved from this investigation demonstrated that the biochar derived from five macroalgae biomass samples have distinguished properties for potential applications in many areas, including adsorption, soil amendment, catalyst, energy storage and soil fertility. In this study, all biochar samples showed exceptional methylene blue adsorption efficiency ranging from 95% to 100%. The current investigation suggested that biochar

preparation techniques and characterization are vital to understanding physical and chemical properties for specific applications. Further research on macroalgal biochar is in progress for their applications across various industries.

Authors' contributions

AKM and UK conceptualised and designed the project. UK and PR took care of project administration, providing research resources, supervision, and validation of the research. Biochar synthesis, characterization and data analysis were done by AKM. ICP-MS and MP-AES was conducted by CH. AKM took the lead in writing the manuscript. All authors provided critical feedback and helped to shape the research, analysis, and manuscript review and editing. All authors read and approved the final manuscript.

Conflicts of interest

There are no conflicts to declare.

References

1 J. Sun, O. Norouzi and O. Mašek, *Bioresour. Technol.*, 2022, **346**, 126258.
2 Y. Xie, L. Wang, H. Li, L. J. Westholm, L. Carvalho, E. Thorin, Z. Yu, X. Yu and Ø. Skreiberg, *J. Anal. Appl. Pyrolysis*, 2022, **161**, 105405.
3 P. Wu, Z. Wang, N. S. Bolan, H. Wang, Y. Wang and W. Chen, *Biochar*, 2021, **3**, 419–436.
4 X. Xiao, B. Chen, Z. Chen, L. Zhu and J. L. Schnoor, *Environ. Sci. Technol.*, 2018, **52**, 5027–5047.
5 X. Tan, Y. Liu, G. Zeng, X. Wang, X. Hu, Y. Gu and Z. Yang, *Chemosphere*, 2015, **125**, 70–85.
6 S. Rawat, C.-T. Wang, C.-H. Lay, S. Hotha and T. Bhaskar, *J. Energy Storage*, 2023, **63**, 107115.
7 D. Mohan, A. Sarswat, Y. S. Ok and C. U. Pittman Jr, *Bioresour. Technol.*, 2014, **160**, 191–202.
8 K. G. Roberts, B. A. Gloy, S. Joseph, N. R. Scott and J. Lehmann, *Environ. Sci. Technol.*, 2010, **44**, 827–833.
9 T. Chopin and A. G. J. Tacon, *Rev. Fish. Sci.*, 2021, **29**, 139–148.
10 R. Gurav, S. K. Bhatia, T.-R. Choi, Y.-K. Choi, H. J. Kim, H.-S. Song, S. M. Lee, S. L. Park, H. S. Lee and J. Koh, *Chemosphere*, 2021, **264**, 128539.
11 K. Vikrant, K.-H. Kim, Y. S. Ok, D. C. W. Tsang, Y. F. Tsang, B. S. Giri and R. S. Singh, *Sci. Total Environ.*, 2018, **616**, 1242–1260.
12 Z.-q. Hou, M.-y. Luo, Y.-t. Yang, J.-c. Zhou, L.-c. Liu and J.-j. Cai, *New. Carbon Mater.*, 2021, **36**, 278–303.
13 M. I. Bird, C. M. Wurster, P. H. de Paula Silva, A. M. Bass and R. De Nys, *Bioresour. Technol.*, 2011, **102**, 1886–1891.
14 K.-W. Jung, K. Kim, T.-U. Jeong and K.-H. Ahn, *Bioresour. Technol.*, 2016, **200**, 1024–1028.
15 L. Mata, A. Schuenhoff and R. Santos, *J. Appl. Phycol.*, 2010, **22**, 639–644.
16 E. Singh, R. Mishra, A. Kumar, S. K. Shukla, S.-L. Lo and S. Kumar, *Process Saf. Environ. Prot.*, 2022, **163**, 585–600.
17 H. Lyu, Y. Gong, R. Gurav and J. Tang, in *Biochar Application*, Elsevier, 2016, pp. 221–246.
18 W. Gao, K. Chen, J. Zeng, J. Xu and B. Wang, *Bioresour. Technol.*, 2017, **243**, 212–217.
19 A. Demirbas, *J. Anal. Appl. Pyrolysis*, 2004, **72**, 243–248.
20 N. T. L. Chi, S. Anto, T. S. Ahamed, S. S. Kumar, S. Shanmugam, M. S. Samuel, T. Mathimani, K. Brindhadevi and A. Pugazhendhi, *Fuel*, 2021, **287**, 119411.
21 N. Canabarro, J. F. Soares, C. G. Anchieta, C. S. Kelling and M. A. Mazutti, *Sustainable Chem. Processes*, 2013, **1**, 1–10.
22 S. E. Kolb, K. J. Fermanich and M. E. Dornbush, *Soil Sci. Soc. Am. J.*, 2009, **73**, 1173–1181.
23 J. Sun, F. He, Y. Pan and Z. Zhang, *Acta Agric. Scand. Sect. B Soil Plant Sci*, 2017, **67**, 12–22.
24 A. Anand, S. Gautam and L. C. Ram, *J. Anal. Appl. Pyrolysis*, 2023, **170**, 105881.
25 Y. Shinogi and Y. Kanri, *Bioresour. Technol.*, 2003, **90**, 241–247.
26 O. Mašek, P. Brownsort, A. Cross and S. Sohi, *Fuel*, 2013, **103**, 151–155.
27 J. J. Manyà, *Environ. Sci. Technol.*, 2012, **46**, 7939–7954.
28 M. K. Hossain, V. Strezov, K. Y. Chan, A. Ziolkowski and P. F. Nelson, *J. Environ. Manag.*, 2011, **92**, 223–228.
29 Z. Wang, K. Liu, L. Xie, H. Zhu, S. Ji and X. Shu, *J. Anal. Appl. Pyrolysis*, 2019, **142**, 104659.
30 X. J. Lee, H. C. Ong, Y. Y. Gan, W.-H. Chen and T. M. I. Mahlia, *Energy Convers. Manage.*, 2020, **210**, 112707.
31 Y.-D. Chen, F. Liu, N.-Q. Ren and S.-H. Ho, *Chin. Chem. Lett.*, 2020, **31**, 2591–2602.
32 O. Farobie, A. Amrullah, A. Bayu, N. Syaftika, L. A. Anis and E. Hartulistiyoso, *RSC Adv.*, 2022, **12**, 9567–9578.
33 A. Sluiter, B. Hames, R. Ruiz, C. Scarlata, J. Sluiter, D. Templeton and D. Crocker, *Laboratory analytical procedure*, 2008, **1617**, 1–16.
34 Y. Zhang, H. Wang, X. Sun, Y. Wang and Z. Liu, *BioResources*, 2021, **16**, 7205.
35 C. Ververis, K. Georghiou, D. Danielidis, D. G. Hatzinikolaou, P. Santas, R. Santas and V. Corleti, *Bioresour. Technol.*, 2007, **98**, 296–301.
36 T. Fazal, A. Faisal, A. Mushtaq, A. Hafeez, F. Javed, A. Alaud Din, N. Rashid, M. Aslam, M. S. U. Rehman and F. Rehman, *Biomass Convers. Biorefin.*, 2021, **11**, 1491–1506.
37 S. M. Renaud, J. T. Luong-Van, D. Dickinson and W. Prins, *J. Appl. Phycol.*, 2006, **18**, 381–387.
38 A. B. Ross, J. M. Jones, M. L. Kubacki and T. Bridgeman, *Bioresour. Technol.*, 2008, **99**, 6494–6504.
39 A. Tomczyk, Z. Sokołowska and P. Boguta, *Rev. Environ. Sci. Bio/Technol.*, 2020, **19**, 191–215.
40 F. Ronsse, S. Van Hecke, D. Dickinson and W. Prins, *GCB Bioenergy*, 2013, **5**, 104–115.
41 K. Jindo, H. Mizumoto, Y. Sawada, M. A. Sanchez-Monedero and T. Sonoki, *Biogeosciences*, 2014, **11**, 6613–6621.
42 M. I. Bird, C. M. Wurster, P. H. de Paula Silva, N. A. Paul and R. De Nys, *GCB Bioenergy*, 2012, **4**, 61–69.

43 D. Özçimen and A. Ersoy-Meriçboyu, *Renewable energy*, 2010, **35**, 1319–1324.
44 S. Wang, G. Dai, H. Yang and Z. Luo, *Prog. Energy Combust. Sci.*, 2017, **62**, 33–86.
45 A. T. Tag, G. Duman, S. Ucar and J. Yanik, *J. Anal. Appl. Pyrolysis*, 2016, **120**, 200–206.
46 A. Petrovič, S. Vohl, T. Cenčič Predikaka, R. Bedoić, M. Simonič, I. Ban and L. Čuček, *Sustainability*, 2021, **13**, 9642.
47 J. E. Kim, S. K. Bhatia, H. J. Song, E. Yoo, H. J. Jeon, J.-Y. Yoon, Y. Yang, R. Gurav, Y.-H. Yang and H. J. Kim, *Bioresour. Technol.*, 2020, **306**, 123092.
48 B. Chen, Z. Gu, M. Wu, Z. Ma, H. R. Lim, K. S. Khoo and P. L. Show, *Biomass Bioenergy*, 2022, **167**, 106650.
49 Y. Y. Teh, K. T. Lee, W.-H. Chen, S.-C. Lin, H.-K. Sheen and I. S. Tan, *Bioresour. Technol.*, 2017, **246**, 20–27.
50 A. N. Roslee and N. F. Munajat, *J. Teknol.*, 2018, **80**, 123–130.
51 W. Peng, Q. Wu and P. Tu, *J. Appl. Phycol.*, 2001, **13**, 5–12.
52 A. Agrawal and S. Chakraborty, *Bioresour. Technol.*, 2013, **128**, 72–80.
53 A. T. Koçer and D. Özçimen, *Biomass Convers. Biorefin.*, 2021, 1–10.
54 M. Maaz, M. Aslam, M. Yasin, A. L. Khan, A. Mushtaq, T. Fazal, A. M. Aljuwayid, M. A. Habila and J. Kim, *Chemosphere*, 2023, **324**, 138197.
55 C.-M. Hung, C. P. Huang, S.-L. Hsieh, M.-L. Tsai, C.-W. Chen and C.-D. Dong, *Chemosphere*, 2020, **254**, 126916.
56 B. Cao, J. Yuan, D. Jiang, S. Wang, B. Barati, Y. Hu, C. Yuan, X. Gong and Q. Wang, *Fuel*, 2021, **285**, 119164.
57 K. K. Jaiswal, V. Kumar, M. S. Vlaskin, M. Nanda, M. Verma, W. Ahmad and H. Kim, *Environ. Technol. Innovation*, 2021, **22**, 101440.
58 J. J. Zhao, X. J. Shen, X. Domene, J. M. Alca Niz, X. Liao and C. Palet, *Sci. Rep.*, 2019, **9**, 1–12.
59 J. Jiang, W. Yang, Y. Cheng, Z. Liu, Q. Zhang and K. Zhao, *Fuel*, 2019, **239**, 559–572.
60 Z. Ding, Y. Wan, X. Hu, S. Wang, A. R. Zimmerman and B. Gao, *J. Ind. Eng. Chem.*, 2016, **37**, 261–267.
61 J. McDonald-Wharry, M. Manley-Harris and K. Pickering, *Carbon*, 2013, **59**, 383–405.
62 A. C. Ferrari and D. M. Basko, *Nat. Nanotechnol.*, 2013, **8**, 235–246.
63 Y.-R. Rhim, D. Zhang, D. H. Fairbrother, K. A. Wepasnick, K. J. Livi, R. J. Bodnar and D. C. Nagle, *Carbon*, 2010, **48**, 1012–1024.
64 Y. Zhou, Z. Li, L. Ji, Z. Wang, L. Cai, J. Guo, W. Song, Y. Wang and A. M. Piotrowski, *J. Mol. Liq.*, 2022, **353**, 118623.
65 A. Mukherjee, R. Lal and A. R. Zimmerman, *Sci. Total Environ.*, 2014, **487**, 26–36.
66 K.-M. Poo, E.-B. Son, J.-S. Chang, X. Ren, Y.-J. Choi and K.-J. Chae, *J. Environ. Manag.*, 2018, **206**, 364–372.
67 X. Xiao, Z. Chen and B. Chen, *Sci. Rep.*, 2016, **6**, 22644.
68 Z. Chang, L. Tian, J. Zhang and D. Zhou, *Ecotoxicol. Environ. Saf.*, 2022, **238**, 113598.
69 M. Z. Yameen, H. AlMohamadi, S. R. Naqvi, T. Noor, W.-H. Chen and N. A. S. Amin, *Fuel*, 2023, **337**, 127215.
70 T. A. T. Yasim-Anuar, L. N. Yee-Foong, A. A. Lawal, M. A. A. Farid, M. Z. M. Yusuf, M. A. Hassan and H. Ariffin, *RSC Adv.*, 2022, **12**, 13938–13949.
71 N. Bolan, S. A. Hoang, J. Beiyuan, S. Gupta, D. Hou, A. Karakoti, S. Joseph, S. Jung, K.-H. Kim and M. B. Kirkham, *Int. Mater. Rev.*, 2022, **67**, 150–200.
72 C. Echeverria, F. Pahlevani, V. Gaikwad and V. Sahajwalla, *J. Cleaner Prod.*, 2017, **154**, 284–294.
73 I. G. Edeh, O. Mašek and W. Buss, *Sci. Total Environ.*, 2020, **714**, 136857.
74 H. Parsimehr and A. Ehsani, *Green Chem.*, 2020, **22**, 8062–8096.
75 K. B. Cantrell, P. G. Hunt, M. Uchimiya, J. M. Novak and K. S. Ro, *Bioresour. Technol.*, 2012, **107**, 419–428.
76 X. Cao, L. Ma, B. Gao and W. Harris, *Environ. Sci. Technol.*, 2009, **43**, 3285–3291.
77 U. Ibi, 2015.
78 H. Ebc, European Biochar Fondation (EBC), Arbaz, Switzerland, 2012.